Title: Obesity-associated inflammation promotes angiogenesis and breast cancer via angiopoietin-like 4

Authors: Ryan Kolb[1,2,*], Paige Kluz[1,3], Zhen Wei Tan[4], Nicholas Borcherding [1,5,6], Nicholas Bormann[7], Ajaykumar Vishwakarma[1,6], Louis Balcziak[8], Pengcheng Zhu[4], Brandon SJ. Davies[9], Francoise Gourronc[10], Ling-Zhi Liu[1], Xin Ge[1], Bing-Hua Jiang[1], Katherine Gibson-Corley[1], Aloysius Klingelhutz[10], Nguan Soon Tan[4,11,12,13], Yuwen Zhu[14], Fayyaz S. Sutterwala[15], Xian Shen[16,*], Weizhou Zhang[1,3,5,6,*].

[1.] Department of Pathology, University of Iowa Carver College of Medicine, Iowa City, IA 52242

[2.] Center for immunology and immune based diseases, University of Iowa Carver College of Medicine, Iowa City, IA 52242

[3.] Free Radical and Radiation Biology, University of Iowa Carver College of Medicine, Iowa City, IA 52242

[4.] School of Biological Sciences, Nanyang Technological University, 60 Nanyang Drive, Singapore 637551

[5.] Medical Scientist Training Program, University of Iowa Carver College of Medicine, Iowa City, IA 52242

[6.] Cancer Biology Graduate Program, University of Iowa Carver College of Medicine, Iowa City, IA 52242

[7.] Department of Psychiatry, University of Iowa Carver College of Medicine, Iowa City, IA 52242.

[8.] Interdisciplinary Neuroscience graduate program, University of Iowa Carver College of Medicine, Iowa City, IA 52242

[9.] Department of Biochemistry, Fraternal Order of Eagles Diabetes Research Center, and Obesity Research and Education Initiative, University of Iowa, Iowa City, IA 52242

[10.] Department of Microbiology and Immunology, University of Iowa Carver College of Medicine, Iowa City, IA, 52242

[11.] Lee Kong Chian School of Medicine, Nanyang Technological University, 50 Nanyang Drive, Singapore 639798

[12.] Institute of Molecular Cell Biology, 61 Biopolis Drive, Proteos, Agency for Science Technology & Research, Singapore 138673

[13.] KK Research Centre, KK Women's and Children Hospital, 100 Bukit Timah Road, Singapore 229899

[14.] Department of Surgery, University of Colorado, Denver/Anschutz Medical Campus, Aurora, CO 80045

[15.] Department of Medicine, Cedars- Sinai Medical Center, Los Angeles, CA 90048

[16.] Division of Gastrointestinal Surgery, the Second Affiliated Hospital of Wenzhou Medical University, Zhejiang, 325035, China

Running Title: ANGPTL4 in obesity-driven breast cancer

Financial Support: RK: NIH T32 AI007260; WZ: NIH R01 grants CA200673 and CA203834, Oberley Award (National Cancer Institute Award P30CA086862) from Holden Comprehensive Cancer Center at the University of Iowa; NB: NIH F30 CA206255; AK: Mark Stinski Developmental Grant from the Department of Microbiology, University of Iowa; BD: NIH R01HL130146; NST: grant from Ministry of Education, Singapore (MOE2014-T2-1-012); FSS: NIH R01 AI118719.

* Corresponding Authors:

Weizhou Zhang. Phone: 01-319-335-8214. FAX: 319-3358453. Email: weizhou-zhang@uiowa.edu

Xian Shen. Phone: 86-577-8800-2501. Email: shenxian1120@126.com

Ryan Kolb. Phone: 01-319-335-6832. Email: ryan-kolb@uiowa.edu

Abstract

Obesity is a risk factor for breast cancer and also predicts poor clinical outcomes regardless of menopausal status. Contributing to the poor clinical outcomes is the suboptimal efficacy of standard therapies due to dose limiting toxicities and obesity related complications, highlighting the need to develop novel therapeutic approaches for treating obese patients. We recently found that obesity leads to an increase in tumor-infiltrating macrophages with activated NLRC4 inflammasome and increased interleukin (IL)-1β production. IL-1β, in turn, leads to increased angiogenesis and cancer progression. Using Next Generation RNA sequencing, we identified an NLRC4/IL-1β-dependent upregulation of angiopoietin-like 4 (ANGPTL4), a known angiogenic factor in cancer, in tumors from obese mice. ANGPTL4-deficiency by genetic knockout or treatment with a neutralizing antibody led to a significant reduction in obesity-induced angiogenesis and tumor growth. At a mechanistic level, ANGPTL4 expression is induced by IL-1β from primary adipocytes in a manner dependent on NF-κB- and MAP kinase-activation, which is further enhanced by hypoxia. This report shows that adipocyte-derived ANGPTL4 drives disease progression under obese conditions and is a potential therapeutic target for treating obese breast cancer patients.

Key Words: Breast cancer/obesity/inflammation/ANGPTL4/Angiogenesis

Introduction

Obesity is associated with an increased risk of estrogen receptor-positive breast cancer in postmenopausal women and a worse clinical outcome regardless of menopausal status[1]. While outcomes for obese patients are worse, treatment options are the same despite often being less efficacious due to dose limiting toxicities and obesity-related complications, thus underlying the need to develop specific therapies for better treating obese patients. We recently found that obesity promotes breast cancer progression by inducing the activation of NLRC4 inflammasome and the consequent IL-1β production from macrophages. IL-1β then promotes angiogenesis and disease progression[2]. An association between obesity and increased tumor angiogenesis has been reported in several other studies[3-5], underscoring the potential importance of increased angiogenesis to obesity-driven breast cancer progression.

Antiangiogenic therapies have been approved for use in several types of cancer; however, survival benefits have been minimal[6]. In breast cancer, the anti-vascular endothelial growth factor (VEGF) antibody, bevacizumab, failed approval following phase 3 clinical trials due to a lack of overall survival benefits[7]. Thus, identifying patients which may benefit from anti-angiogenic therapies and understanding mechanisms of resistance is important. Studies have shown that anti-VEGF therapies may be beneficial in breast cancer patients with high levels of vascular density. Obese breast cancer patients may represent one such cohort that may respond to anti-angiogenic therapies. However, obesity may promote resistance to ani-VEGF therapy[8].

Angiopoietin-like 4 (ANGPTL4) is a secreted protein that is cleaved into two active peptides[9]. The N-terminus domain is a potent inhibitor of lipoprotein lipase (LPL) activity and modulates lipid composition and energy homeostasis[9]. The C-terminus (cANGPTL4) domain is involved in wound healing, vessel permeability, and angiogenesis[10]. ANGPTL4 plays a role in promoting the progression of several types of cancer[11, 12] and is correlated with poor response to anti-VEGF therapy[13]. Here we show that obesity-associated NLRC4 inflammasome activation/IL-1β leads to the upregulation of ANGPTL4, primarily in adipocytes. This increase in ANGPTL4 is required for obesity-driven breast cancer progression and angiogenesis and targeting cANGPTL4 with a neutralizing antibody inhibits obesity-driven tumor progression.

Results

Obesity-associated NLRC4-inflammasome activation/IL-1β upregulates *Angptl4*

We recently found that obesity promotes breast cancer progression via NLRC4-inflammasome activation and subsequent IL-1β secretion in tumor-infiltrating macrophages[2]. To further understand how NLRC4-inflammasome promotes cancer progression, we performed Next Generation RNA sequencing on Py8119 orthotopic tumors from wild-type (wt) mice given a normal diet (ND), WT mice with high-fat diet (HFD), or the HFD-fed *Nlrc4*$^{-/-}$ mice used in our previous study[2]. Using the criterion described in the materials and methods, we identified 8 genes that were upregulated in an NLRC4-dependent manner in tumors from obese mice and 10 that were downregulated (Figure 1A). Among the most highly upregulated genes was *Angptl4*, whose expression was further verified by real-time PCR showing an increase in Py8119 (Figure 1B) and E0771 (Figure 1C) tumors from obese mice but not in those from obese NLRC4 inflammasome-deficient mice (*Nlrc4*$^{-/-}$ HFD and *Casp1/11*$^{-/-}$HFD, the common effector enzyme for inflammasomes).

ANGPTL4 promotes obesity-driven breast cancer progression and angiogenesis

To determine if ANGPTL4 plays a role in obesity-driven breast cancer progression, we fed *Angptl4*$^{-/-}$ and *Angptl4*$^{+/-}$ littermates an ND or HFD for 10 weeks prior to implantation of Py8119 cells. We observed no significant difference in weight gain between the *Angptl4*$^{-/-}$ and *Angptl4*$^{+/-}$ mice (Figure 2A). Tumor growth in *Angptl4*$^{+/-}$ mice fed with the HFD was significantly higher than that in *Angptl4*$^{+/-}$ mice fed with ND (Figure 2B). This obesity-driven tumor progression was significantly reduced in *Angptl4*$^{-/-}$ mice (Figure 2B). Tumor growth in *Angptl4*$^{-/-}$ mice fed HFD was similar to that of *Angptl4*$^{+/-}$ and *Angptl4*$^{-/-}$ mice fed ND, suggesting that only in the obese setting is tumor growth dependent on ANGPTL4. We next verified the role of ANGPTL4 in obesity-driven breast cancer progression using E0771 breast cancer cells and found similar results (Figure 2C). Obesity led to an increase in tumor growth in WT mice and was partially, but significantly, reduced (P=0.016) in obese *Angptl4*-

deficient mice (Figure 2C). These data support that the upregulation of ANGPTL4 is critical in promoting cancer progression under obesity.

It has been previously reported that *Angptl4*$^{-/-}$ mice given a diet high in saturated fatty acids, such as the one used in our studies, have a systemic inflammatory response eventually leading to intestinal fibrosis and cachexia[14]. The authors noted that *Angptl4*$^{-/-}$ mice given a diet high in unsaturated fatty acids did not present any of these clinical abnormalities. To determine if this inflammatory response may effect tumor growth in our model, we fed WT and *Angptl4*$^{-/-}$ mice a safflower oil-based HFD consisting of primarily 18:2 unsaturated fatty acids (HFD-Saff); however, the *Angptl4*$^{-/-}$ mice failed to gain weight making this an inappropriate model to study obesity-driven breast cancer progression (Supplementary Figure S1A). This lack of weight gain from 18:2 unsaturated fatty acids is an intriguing future avenue of investigation for ANGPTL4's role in regulation of LPL. Furthermore, tumors from *Angptl4*$^{-/-}$ mice given a HFD had similar numbers of tumor-infiltrating macrophages and IL-1β levels as those in *Angptl4*$^{+/-}$ mice (Supplementary Figure S1B-D).

In our previous study, we found that NLRC4-inflammasome promotes tumor angiogenesis in obese mice[2]. As previous studies have shown that ANGPTL4 can promote angiogenesis[15], we next determined if upregulation of ANGPTL4 in obese mice led to increased angiogenesis. Immunohistochemical staining for CD31, a marker for endothelial cells, showed a significant increase in CD31-positive staining in tumors from *Angptl4*$^{+/-}$ HFD mice compared to *Angptl4*$^{+/-}$ ND mice (Figure 2D-E). This increase in CD31-positive staining was partially reduced in *Angptl4*$^{-/-}$ HFD mice, suggesting that obesity-driven tumor angiogenesis is at least partially dependent on ANGPTL4. While obese *Angptl4*$^{-/-}$ mice had increased CD31 staining compared to *Angptl4*$^{+/-}$ or *Angptl4*$^{-/-}$ ND mice, the difference was not significant (Figure 2D-E). Similar results were found using a second endothelial cell marker, CD34, wherein tumors from obese wild-type mice had increased CD34-positive staining compared to ND mice but not in those from obese ANGPTL4-deficient mice (Figure 2F-G). In Figure 2D-G, the tumors were collected at the same time and hence the tumors from the HFD group were larger (Figure 2B). To determine if this difference in size played a role in the increased angiogenesis, we collected tumors from ND and HFD mice when they reached 2 cm in diameter and stained for CD31. Tumors from obese mice still had increased CD31 staining

compared to tumors from ND mice, indicating that the difference in angiogenesis was not due to the larger tumors (Supplementary Figure S2A). This ANGPTL4-dependent increase in angiogenesis was also seen in E0771 tumors (Figure 2H-I), further supporting the role of obesity-associated ANGPTL4 in promoting tumor angiogenesis. We also stained tumor sections for Ki-67, a proliferation marker, and found no difference between tumors from obese and ND mice (Supplementary Figure S2B).

IL-1β promotes the upregulation of *Angptl4* in adipocytes

To determine the source of ANGPTL4 in response to IL-1β in obese tumor, we treated various cell types found in the tumor microenvironment with IL-1β and measured *Angptl4* expression. IL-1β did not induce *Angptl4* expression in Py8119 cancer cells, bone-marrow-derived macrophages (BMDM, Mφ), cancer-associated fibroblasts (CAFs), or endothelial cells (SVEC; Figure 3A). In contrast, IL-1β induced a significant, 28-fold increase in *Angptl4* mRNA in primary mouse adipocytes (Figure 3A). It should also be noted that the relative expression of *Angptl4* is 200x or higher in primary adipocytes than in the other cell types tested (Figure 3A). The high expression of *Angptl4* in mouse adipocytes corresponds with RNA-sequencing data from human tissues showing that adipose tissue has the highest expression of *ANGPTL4* (Supplementary Figure S3A). Western Blotting analysis of whole cell lysates and media from human adipocytes, obtained by differentiation of an immortalized preadipocyte cell line[18], showed that IL-1β induced ANGPTL4 protein in human adipocytes mainly as the secreted form in media (Figure 3B). Adipocytes are an important cell type in the breast tumor microenvironment[16] and are frequently found in mammary tumors. The number of adipocytes was increased in tumors from obese mice regardless of whether ANGPTL4 was present (Supplementary Figure S3B-C). The high expression of ANGPTL4 in primary adipocytes compared to other stromal cells indicates that ANGPTL4 is primarily produced from adipocytes in the obese microenvironment. To determine which signaling pathway is involved in the upregulation of *Angptl4*, we treated adipocytes with IL-1β in the presence or absence of either an NF-κB- or a JNK-inhibitor. Inhibition of NF-κB partially reduced IL-1β-induced upregulation of *Angptl4* expression in primary adipocytes, while inhibition of JNK attenuated IL-1β-induced *Angptl4* (Figure 3C),

157 suggesting that ANGPTL4 expression is induced through NF-κB- and JNK-mediated signaling pathways. We
158 also treated primary mouse adipocytes with IL-1β in the presence or absence of D-JNKi, a cell-permeable peptide
159 inhibitor of JNK[17], or control peptide and confirmed that inhibition of JNK signaling abolished IL-1β-induced
160 *Angptl4* (Figure 3D). The inhibition of IL-1β-induced JNK activation was confirmed by Western Blotting for
161 phospho-c-JUN downstream of JNK activation (Supplementary Figure 3D). We transduced differentiated human
162 adipocytes with adenovirus expressing GFP (Ad-GFP), dominant-negative (DN) JNK (Ad-DN-JNK) or DN
163 IKKβ (Ad-DN-IKKβ), following with IL-1β treatment. Infectivity was verified by expression of GFP
164 (Supplementary Figure S3E). IL-1β-induced expression *ANGPTL4* in human adipocytes was inhibited by the
165 expression of DN JNK and DN IKKβ (Figure 3E), further confirming the role of NF-κB- and JNK-mediated
166 signaling in the regulation of ANGPTL4 downstream of IL-1β.

167 ANGPTL4 is a known to be regulated by hypoxia-inducible factor 1 (HIF1)[19]. We stained tumor sections
168 with HIF1α and counted the number of cells with nuclear HIF1α staining as a marker for hypoxia. While we
169 didn't see an increase in nuclear HIF1α staining in tumors from obese mice, both the tumor microenvironment
170 and obese adipose tissues tend to have regional hypoxia (Supplementary Figure S3F-G). We hence determined the
171 effect of hypoxia on IL-1β-induced *Angptl4*. While both hypoxia (incubation of cells at 1% O_2) and IL-1β
172 induced the expression of *Angptl4*, the combination of IL-1β and hypoxia induced a further upregulation of
173 *Angptl4* relative to either alone: 4.7-fold increase over hypoxia alone and 11.1-fold increase over IL-1β alone
174 (Figure 3F). Human adipocytes were treated as in Figure 3F and similar to mouse adipocytes, hypoxia induced a
175 significant increase in *ANGPTL4* expression, which is further increased by IL-1β (Figure 3G). We previously
176 showed that vascular endothelial growth factor (VEGF) A is upregulated by IL-1β in obese tumors in our model[2].
177 As such, we examined the IL-1β induced *Vegfa* in adipocytes in conjunction with hypoxia. In primary adipocytes,
178 while both IL-1β and hypoxia induced *Vegfa* expression individually, the combination did not significantly
179 increase its expression compared to hypoxia alone (Supplementary Figure S3H). These data indicate that the
180 upregulation of IL-1β in obese tumors acts collectively with hypoxia to induce *Angptl4* expression in adipocytes.

ANGPLT4 in human obesity and breast cancer

We next examined the relevance of ANGPTL4 in human obesity and breast cancer. Analysis of the publicly available dataset (GSE33256) showed a significant increase in the expression of *ANGPTL4* in normal breast tissue from obese women compared to normal weight women (Figure 4A). Using a meta-dataset with 2315 samples, we found that *ANGPTL4* expression was inversely correlated with recurrence-free survival (RFS; hazard ratio HR=1.3) across all breast cancer subtypes (Figure 4B), which became much more pronounced within basal-like breast cancer (HR=2.05; Figure 4C). Examining TCGA breast cancer expression data, we also found that *ANGPTL4* expression was highest in aggressive basal-like breast cancer compared to Luminal A, Luminal B, and HER2 subtypes (Figure 4D).

We analyzed basal-like breast cancers as they had the highest expression of *ANGPTL4*, and found that there is a positive correlation between *ANGPTL4* and *PECAM1* (CD31) (Figure 4E), suggesting that ANGPTL4 is positively correlated with angiogenesis in human breast cancer. Using a publically available dataset of 198 basal-like breast cancer samples (GSE76275), we performed Gene Set Enrichment Analysis (GSEA) comparing transcriptomes with high expression of *ANGPTL4* versus those with low expression of *ANGPTL4*, to identify pathways and gene sets associated with *ANGPTL4*. We found an enrichment for gene sets related to all of the ANGPTL4 regulatory pathways, including those of hypoxia and HIF signaling, IL-1 signaling, JNK signaling, NFκB signaling, and PPAR/Adipogenesis (Figure 4F, Supplementary Table 1). We also found the enrichment for gene sets related to angiogenesis and obesity, further corroborating an association between ANGPTL4, obesity and angiogenesis in breast cancer (Figure 4F, Supplementary Table 1). We previously reported an upregulation of *VEGFA* in response to NLRC4 inflammasome/IL-1β[2]. We also determined if *VEGFA* was associated with enrichment for gene sets related to the same pathways associated with *ANGPTL4* expression. While high *VEGFA* expression was associated with fewer pathways overall compared to pathways altered in high *ANGPTL4* specimens, *VEGFA* expression was associated with enrichment for pathways related to Hypoxia/HIF signaling as well as NFκB and PPAR/adipogenesis, but not pathways related to JNK, IL-1 or obesity (Supplementary Figure

S4A, Supplementary Table 2). As expected, cancer specimens with high expression of *VEGFA* exhibited enrichment for gene sets related to angiogenesis and VEGFA signaling (Supplementary Figure S4A, Supplementary Table 2). We also found that cancer specimens with high expression of *ANGPTL4* had enrichment for gene sets related to the same pathways, regardless of whether the samples were first separated into groups with high or low expression of *VEGFA* (Figure 4F, Supplementary Figure S4B, Supplementary Tables 3-4), suggesting that expression of *ANGPTL4* is associated with these pathways independently of *VEGFA* expression. Previous studies have found that both VEGFA and ANGPTL4 are required for angiogenesis[19] in certain situations and that high expression of *ANGPTL4* is correlated with poor response to anti-VEGF therapies[13]. Interestingly, we found a body-mass index (BMI)-dependent correlation pattern between *VEGFA* and *ANGPTL4*, with significant correlation between *VEGFA* and *ANGPTL4* expression (Pearson r=0.43) in obese breast cancer patients, a trend to positive correlation in overweight patients (Pearson r=0.24), and no correlation in normal weight patients (Figure 4G). These analyses suggest that ANGPTL4 and VEGF cooperatively promote angiogenesis in obese patients.

Targeting cANGPTL4 inhibits obesity-driven breast cancer progression

To see if targeting ANGPTL4 would inhibit obesity-driven breast cancer progression, we used a neutralizing antibody against the C-terminus of ANGPTL4[20, 21]. Mice were given either a ND or HFD for 10 weeks then implanted with Py8119 cells as in Figure 2. Once tumors were palpable, the mice were treated with the anti-cANGPTL4 blocking antibody or IgG as a control (Figure 5A). Blocking cANGPTL4 reduced obesity-driven tumor growth compared to obese mice treated with IgG control (Figure 5A). Anti-cANGPTL4 antibody treatment in mice fed ND had no effect on tumor growth (Figure 5A). Treating obese mice with anti-cANGPTL4 antibody also reduced tumor angiogenesis indicated by CD31 IHC staining as compared to obese mice treated with IgG, though the difference was barely insignificant (Figure 5B-C). This data indicates that targeting cANGPTL4 with a neutralizing antibody can inhibit obesity-driven breast cancer progression and angiogenesis.

We had 5 monoclonal antibodies against human cANGPTL4 developed which bound to both denatured and folded human cANGPTL4. To determine if these antibodies could block cANGPTL4 function, we performed

an endothelial cell tube formation assay[22]. Treatment of endothelial cells with recombinant human cANGPTL4 induced tube formation (Figure 5D-E). cANTPTL4-induced tube formation was inhibited by co-treating cells with antibodies targeting human cANGPTL4 (Figure 5D-E). Importantly, these antibodies did not inhibit serum-induced tube formation (Figure S5). We next performed an *in vivo* matrigel plug assay using hemoglobin as a readout for angiognesis[23]. As shown in Figure 5F-G, recombinant cANGPTL4 induced angiogenesis in a dose dependent manner in matrigel plugs from athymic nude mice (Figure 5F, middle two panels Vs control panel) and quantitated by hemoglobin protein expression (Figure 5G, bar 1, 2, and 4). The cANGPTL4-induced angiogenesis *in vivo* was completely blocked by treatment with our new anti-cANGPTL4 antibody (Figure 5F, right two panels Vs middle two panels) and further quantitated by hemoglobin protein expression (Figure 5G, bar 3 Vs 2 and bar 5 Vs 4). These data indicate that cANGPTL4 can directly induce angiogenesis and can be blocked with anti-ANGPTL4 antibody against cANGPTL4.

Discussion

Previously we showed that obesity-associated NLRC4-inflammasome activation in infiltrating macrophages drove increases in angiogenesis and breast cancer progression[2], suggesting that obese breast cancer patients may represent a patient cohort that might benefit from VEGFA targeted therapy. Bevacizumab (Avastin) is an FDA-approved neutralizing antibody for human VEGFA to treat several solid cancers, but it failed in breast cancer due to lack of overall survival benefit. There is no doubt that angiogenesis is required for tumor growth and progression. Here we identified ANGPTL4, a different angiogenic factor, as critical for angiogenesis under obesity. Obesity is known to be associated with increased VEGFA expression and angiogenesis. As depicted (Supplementary Figure S6), we found much more pronounced increase in ANGTPL4 expression from adipocytes that can be regulated by several pathways: 1) (purple) IL-1β produced by macrophages directly acts on adipocytes and induces *Angptl4* transcription via JNK and NF-κB pathways; and 2) (blue) Hypoxia within tumor microenvironment and obesity synergizes with IL-1β to induce *Angptl4* transcription likely via HIF1α. These multifaceted *Angptl4* regulations further implicate its important role in tumor growth and progression under obesity. Our animal data further demonstrate the critical role of ANGPTL4 in obesity-driven tumor angiogenesis

and growth in two breast cancer models, suggesting that ANGPTL4 is one of the major obesity-induced angiogenic factors downstream of NLRC4-inflammasome activation and IL-1β release from macrophages.

Based on the expression pattern of *ANGPTL4* in human tissues (Supplementary Figure S3A) and the high expression of *Angptl4* in primary adipocytes compared to other stromal cells found in the tumor microenvironment (Figure 3A), we hypothesize that adipocytes are the primary source of ANGPTL4 in the obese breast tumor microenvironment. Moreover, we observed a reduction in obesity-driven breast cancer progression when ANGPTL4 was lost in the microenvironment but intact in the cancer cells (Figure 2), indicating that the source of ANGPTL4 was from the tumor associated stroma. Previous studies have shown that cancer cells express ANGPTL4. In breast cancer, expression of TGFβ can induce expression of *ANGPTL4*, which can promote lung metastasis[12]. Others have shown that ANGPTL4 is expressed in various tumors and the loss of ANGPTL4 in squamous cell carcinoma and melanoma cells can reduce tumor growth in mouse models[24]. However, here we only focused on the relevance of stromal ANGPTL4 and our data indicate that the major source of ANGPTL4 in primary breast cancer under obesity could be adipocytes.

Our current focus is how obesity-associated microenvironment promotes tumor growth and progression. Based on our and others' results, it is likely that hypertrophic adipocytes from obese individuals recruit macrophages via CCL2 production[5]. The activated macrophages produce IL-1β via NLRC4-inflammaome activation, which in turn works on the above pathways to induce ANGPTL4 from adipocytes and consequent angiogenesis. Based on phenotypic resemblance between ANGPTL4-deficiency and NLRC4-inflammasome inactivation, we conclude that ANGPTL4 is the major downstream effector involved in obesity-driven tumor growth. As several mechanisms have been proposed, we reason that angiogenesis is one of the major pathways in the obesity-driven tumor growth as ANGPTL4 is critical in obesity-associated angiogenesis. We cannot exclude other pathways, but relevant to obesity in these models we did not find significant difference in apoptosis (data not shown) and proliferation (Supplementary Figure S2) between tumors from normal weight mice and those from obese mice. Several recent studies have found that ANGPTL4 can promote survival and proliferation of cancer cells through various mechanisms[24-27], providing possible mechanisms how ANGPTL4 promotes cancer

progression that may be irrelevant of obesity. ANGPTL4-deficient mice have a systemic inflammatory response leading to intestinal fibrosis and cachexia when given a HFD that is high in saturated fatty acids, such as the one used in these studies, but not when given a HFD composed primarily of unsaturated fatty acids[14]. This inflammatory response may have an effect on tumor growth in our model. Since ANGPTL4-deficient mice failed to gain weight when given a safflower oil-based HFD consisting of primarily 18:2 unsaturated fatty acid (Supplementary Figure S1A), we cannot conclusively determine what effect, if any, this inflammatory response to a diet high in saturated fatty acids has on obesity-driven tumor growth in our model. However, we saw no difference in the number of tumor infiltrating macrophages and IL-1β between tumors from control HFD mice compared to *Angptl4*$^{-/-}$ HFD mice (Supplementary Figure S1B-D). Furthermore, obesity-associated tumor growth was abrogated by treating mice with a neutralizing antibody targeting cANGPTL4 (Figure 5A), suggesting that this inflammatory response in ANGPTL4-deficient mice was not responsible for the reduced tumor growth observed in obese *Angptl4*$^{-/-}$ mice (Figure 2B-C).

While anti-VEGF therapies have shown little therapeutic promise in breast cancer, they may be beneficial to patients with high levels of neoangiogenesis[28]. Due to the increase in angiogenesis in obesity-associated breast cancer, we have postulated that anti-VEGF therapies may be a viable therapy in obese breast-cancer patients[2]. However, a recent publication found that obesity promotes resistance to anti-VEGF therapies possibly through the upregulation of IL-6 and FGF-2[8]. Here we found that ANGPTL4 is required for obesity-driven breast cancer progression and angiogenesis, and that its expression is inversely correlated with relapse-free survival (Figure 4). Moreover, we found that *VEGFA* and *ANGPTL4* expression are correlated only in obese patients (Figure 4G). Previous studies have shown that expression of ANGPTL4 is correlated with poor response to anti-VEGFA therapies[13]. Thus, the upregulation of ANGPTL4 represents another mechanism for the resistance to anti-VEGF therapies in obese mice reported previously[8]. Therefore, targeting ANGPTL4 alone or in combination with anti-VEGF therapies may be a better potential therapy for obese breast cancer patients. In particular, the high expression in basal-like breast cancer and its secretive nature make ANGPTL4 an ideal target for antibody-based therapy. Indeed, treating mice with a neutralizing antibody against cANGPTL4 inhibits obesity-driven breast

cancer progression in obese mice (Figure 5A), further highlighting the potential of ANGPTL4 as a therapeutic target for obese breast cancer patients. One caveat is the critical role of its N-terminus in inhibiting LPL regulation that could be detrimental for lipid homeostasis if inhibited. It is unknown if antibodies targeting cANGPTL4 deplete the pool of whole length ANGPTL4 leading to a potential reduction of its N-terminal peptide. Further investigations are warranted to address if cANGPTL4 represents a viable target for therapy in particular to obese patients with basal-like breast cancer.

Materials and Methods

Cell lines, primary adipocytes and cell culture

Py8119 and E0771 cells have been described and validated previously[2, 29, 30]. Cancer associated fibroblast cells were described previously[31]. SVEC endothelial cells were purchased from American Type Culture Collection (ATCC)[32]. Cell lines were routinely tested for mycoplasma contamination. Human preadipocytes (Lonza, Basel Switzerland) were immortalized, cultured and differentiated into mature adipocytes as described previously[18]. Primary mouse preadipocytes were isolated from the mammary fat pad of 4 to 6 day old pups and differentiated into mature adipocytes as described previously[33]. For experiments involving treatment with IL-1β, cells were cultured with 100 ng/ml recombinant mouse human IL-1β (R&D Systems, Minneapolis MN) for 6 hours. For co-treatment with IL-1β, adipocytes were treated with 5 μM BMS345541 (Sigma-Aldrich, St. Louis, MO), an NF-κB inhibitor, 40 μM SP600125 (Sigma Aldrich) a JNK inhibitor, 30 μM D-JNKi (GenScript, Pascataway NJ) or 30 μM control peptide (GenScript), 1 hour prior to treatment with IL-1β. For transduction of differentiated human adipocytes, cells were incubated with purified adenovirus expressing GFP, DN JNK (University of Iowa Viral Vector Core) or DN IKKβ for 16 hrs prior to treatment with IL-1β. Each individual experiment involving primary adipocytes were performed using a batch of adipocytes from a single litter of mice plated in triplicate for each experimental group. These experiments were then repeated at least twice using different batches of primary adipocytes.

Mouse colony and orthotopic transplant model

Animal experiments were approved by the University of Iowa Institutional Animal Care and Use Committee (IACUC) and performed in accordance with IACUC guidelines. All mice used were female mice of C57BL/6N background. *Angptl4*$^{-/-}$ (B6;129S5-Angptl4Gt (OST352973)Lex/Mmucd) mice were obtained from the Mutant Mouse Resource and Research Center (mmrrc.org) and backcrossed 10 generations with C57BL/6N background. For Py8119 transplant models, *Angptl4*$^{+/-}$ and *Angptl4*$^{-/-}$ littermates were used. Tumors from *Casp1/11*$^{-/-}$ [34] and *Nlrc4*$^{-/-}$[35] mice were from our previous publication[2]. Athymic nude mice of both genders were purchased from Charles River Laboratories for matrigel plug assays (San Diego, CA).

The orthotopic transplant model was done as described previously[2]. Briefly, 6-week old mice were randomly grouped and given a normal diet provided by our vivarium, or a high fat diet (HFD, 60% kCal from fat, S3282, Bio-Serv, Flemington, NJ) for 10 weeks, then Py8119 or E0771 cells in Matrigel/PBS were implanted into the #4 mammary gland. Experiments were terminated when the largest tumors reached 2 cm in diameter. A custom safflower oil-based HFD (60 kCal from fat) where in the fat content was 76.6% 18:2 fatty acid was obtained from Research Diets Inc. (New Brunswick, NJ). For experiments involving treatment of mice with antibody, mice were treated with 10mg/kg anti-cANGPTL4 or rabbit IgG (BioXcell, West Lebanon, NH) twice weekly by intraperitoneal (*i.p.*) injection once tumors were palpable. The anti-cANGPTL4 antibody was described previously [20, 21]. For inbred mice, we expect to see variability representing ≤ 40% of the mean of each group, thus, a minimum of 5 mice/group was used to exceed a confidence level of 95% for transplant models and repeated. Animal studies were not performed blinded due to the use of different diets and genotypes.

Western blotting and ELISA

For Western blotting analysis, adipocyte cells were lysed with RIPA buffer. Proteins in cell lysates or media were separated by SDS PAGE and detected by immunoblot analysis. The following antibodies were used: phospho-c-JUN (K-M-1, Santa Cruz Biotechnologies, Dallas TX), rat anti-cANGPTL4 clone 6A11A7 (GenScript), and mouse anti-β-Actin (8H10D10, Cell Signaling Technology, Danvers MA). For ELISA, tissue was lysed in buffer

consisting of 100 mM Tris pH 7.4, 150 mM NaCl, 1 mM ethylenediaminetetraacetic acid, 1 mM ethylene glycol-bis(β-aminoethy ether) N, N, N', N'-tetraacetic acid, 1% Triton X-100, and 0.5% sodium deoxycholate plus protease inhibitors. The ELISA was done using the following protein pair: rat anti-mouse IL-1β (30311, R&D Systems, Minneapolis MN) and goat anti-mouse IL-1β biotinylated (polyclonal, R&D). The ELISA was developed using TMB substrate (Thermo Fisher Scientific, Waltham MA).

Immunohistochemistry (IHC)

Tumor sections were preserved in OCT compound, frozen and sectioned. 5 μm thick sections were fixed in 35/65 methanol/acetone. CD31 was detected with anti-mouse CD31 antibody (MEC13.3, Biolegend, San Diego CA). For the remaining IHC staining, Formalin-fixed tissue samples were paraffinized and sectioned by University of Iowa Comparative Pathology Core. Sections were then de-paraffinized in a series of xylene washes and rehydrated with ethanol and water. Antigen retrieval was accomplished by immersing slides in Citrate Buffer pH 6.0 in a decloaker (Biocare Medical, Concord CA). Tissue samples were incubated with 3% hydrogen peroxide followed by blocking with horse serum (Biocare Medical). Slides were then incubated with rabbit anti-mouse Ki-67 antibody (D2H10, Cell Signaling Technology), rat anti-CD34 antibody (MEC14.7, Novus Biologicals, Littleton CO) or rabbit anti-HIF1α (polyclonal, Abcam, Cambridge UK). Slides were then stained with Rat-on-mouse HRP polymer and probe (Biocare,) or secondary rabbit envision (DAKO, Santa Clara CA). The slides were developed with 3,3'-diaminobenzadine (DAB and 0.3% H_2O_2 in PBS) developing buffer, followed by counterstaining with hematoxylin. Positive staining was quantified using *Image J* software. All analysis of IHC was done blinded in regards to group allocation.

Endothelial cell tube formation assay

SVEC cells were serum-starved (0.3% serum) for 12 hrs, prior to plating $2x10^4$ cells in DMEM in a growth factor reduced matrigel (Corning Inc., Corning NY) coated 48-well plate. 3% serum, recombinant human cANGPTl4 antibodies in hybridoma supernatant diluted 1:50 (GenScript, Piscataway NJ), and 20 μg/ml of cANGPTL4 was added to both the matrigel and the cell suspension as indicated. Rat anti-cANGPTL4 monoclonal antibodies were

generated by GenScript against human cANGPTL4 protein. The ability of these proteins to bind to both denatured and folded cANGPTL4 was verified by GenScript by Western blotting after SDS-PAGE and ELISA, respectively. Cells were then incubated for 6 hours at 37°C. Following incubation cells were stained with 2μg/ml Calcein AM (Thermo Fisher Scientific) for 30 minutes followed by visualization using a fluorescent microscope. Tube formation was quantified using *AngioTool* software [36].

Matrigel plug assay

Athymic nude mice (Charles River Laboratories, San Diego, CA) were implanted with 0.4 ml growth factor reduced matrigel/PBS (Corning Inc.) containing the indicated concentration of recombinant human cANGPTL4 (Genescript) and 48 μg/ml rat IgG or purified rat anti-cANGPTL4 antibody clone 6A11A7 (Genescript) or PBS. After 6 days, mice were euthanized and plugs were used for the measurement of hemoglobin content using the Drabkin's reagent kit according to the manufacturer's instructions (Sigma-Aldrich). The concentration of hemoglobin was based on a set of standards.

Real-time PCR and RNA-seq

RNA was isolated using RNeasy Plus Mini Kit (Qiagen, Hilden, Germany). For real-time PCR, cDNA was generated using Superscript III First Strand cDNA Synthesis Kit (ThermoFisher Scientific). mRNA expression was quantified by real-time PCR using a ViiA7 Real-Time PCR System (ThermoFisher Scientific). The following primers for ANGPTL4 were used: for mouse, 5'-GGAAAAGTCCACTGTGCCTC and 5'-TAGATGACCCAGCTGATTG-3'; for human 5'-TAGTCCCACTCTGCCTCTCCC-3' and 5'-GAGTTGGCCCAGCCAGTT-3'. The following primers for mouse *Il1b* were used" 5'-GCAACTGTTCCTGAACTCAACT-3' and 5'- ATCTTTTGGGGTCCGTCAACT-3'. For RNA-seq, samples were submitted to the Iowa Institute of Human Genomics for quality assessment and samples with a RNA Integrity Number score > 8.0 were submitted to the University of Chicago Genomics for singe-end 50bp on the Illumina HiSeq 2000. Data was aligned using the Usegalaxy web platform and TopHat [37-39]. The aligned data was further processed using cufflinks workflow [40]. The raw data were shown as fragments per kilobase of transcript

per million mapped reads (FPKM). Z-scores and fold change were calculated using the resulting expression data converted to Log2 (FPKM+1) values. Due to the small sample size, 2 per group, determining statistical significance for differentially regulated genes was not possible. Instead, differentially regulated genes in tumors from obese that were NLRC4-dependent were identified as genes with a fold change of greater than or equal to |1.8|. The list was further narrowed to only genes that were upregulated in the HFD group and had a Z-score of greater than 0.5 while the Z-score for the other 4 samples (ND and *Nlrc4*$^{-/-}$ HFD) were less than 0.25. For down regulated genes we included samples where the Z-score was less than 0.25 for the HFD samples and greater than 0.5 for the other 4. A heatmap of differentially regulated genes was made using Graphpad Prism Software (Graphpad Software Inc., San Diego, CA).

Survival and transcriptomics analysis

Recurrence-free survival based on the expression of *ANGPTL4* were generated using data from a published meta-dataset of 3554 breast cancer patient specimens and the KMplot online tools [41]. Expression analyses of the TCGA BRCA cohort were performed using the mean-centralized level 3 Illumina HiSeq2000 RNA-seq data separated into PAM50 subtypes. RNA-seq data from 122 human individual representing 32 tissues was obtained from Human Protein Atlas [42] and *ANGPTL4* expression in different tissues was graphed using Graphpad Prism Software (Graphpad Software Inc). Correlation between *ANGPTL4* and *PECAM1* mRNA was generated using Graphpad Prism Software (Graphpad Software Inc) using TCGA BRCA expression data from basal-like PAM50 subtype. GSE33256, GSE20914 and GSE76275 microarray data were obtained from NCBI Geo Datasets. BMI data for GSE20914 was provided by Dr. Sai-Ching Yeung at MD Anderson Cancer Center. For pathway analysis, basal-like breast cancer samples from GSE76275 were separated into high and low expressing tertiles of *ANGPTL4* (probe 221009_s_at) or *VEGFA* (probe 210512_s_at). Further analysis was done by first separating the samples by *VEGFA* expression into high tertile or low tertile, then further separating each group into high and low *ANGPTL4* expressing tertiles. Geneset Enrichment Analysis (Broad Institute of MIT and Harvard, Boston) was used comparing low expressing tertiles to high expressing tertile for each group. Genesets with a false discovery rate (FDR) <0.25 was considered significant enrichment.

Statistical Analysis

All statistical tests are described in the Figure legends. For animal models, statistical significance for body weight and tumor growth was determined by two-way ANOVA. Statistical significance in expression from human microarray or TCGA data was determined by a Welch's t-test. Pearson r is reported for correlation between the expression of two genes. Long-rank test was ued to determine significance for survival curves. All other experiments used a One-way ANOVA with multiple comparisons correction using Dunnett's test to determine significance. P-values of less than 0.05 were considered significant.

Data Availability

The processed RNA-sequencing data shown as fragments per kilobase of transcript per million mapped reads (FPKM) and their original FASTQ files are currently being submitted to GEO datasets.

Acknowledgements

We would like to thank the Comparative Histopathology Core in the Department of Pathology, University of Iowa for the processing of fixed tissue and CD31 immunohistochemistry. We thank Dr. Mikhail Kolonin (UT health science center at Houston) and Dr. Leslie Ellies (UCSD) for sharing E0771 and Py8119 cells, respectively. Financial Support: RK: NIH T32 AI007260; WZ: NIH grant CA200673, the V Scholar award, Oberley Award (National Cancer Institute Award P30CA086862) from Holden Comprehensive Cancer Center at the University of Iowa; NB: NIH F30CA206255; AK: Mark Stinski Developmental Grant from the Department of Microbiology, University of Iowa; BD: NIH R01HL130146; NST: grant from Ministry of Education, Singapore (MOE2014-T2-1-012); FSS: NIH RO1 AI118719.

Conflict of Interest

The authors declare no conflict of interest.

References

1 Kolb R, Sutterwala FS, Zhang W. Obesity and cancer: inflammation bridges the two. Curr Opin Pharmacol 2016; 29: 77-89.

2 Kolb R, Phan L, Borcherding N, Liu Y, Yuan F, Janowski AM *et al*. Obesity-associated NLRC4 inflammasome activation drives breast cancer progression. Nat Commun 2016; 7: 13007.

3 Gu JW, Young E, Patterson SG, Makey KL, Wells J, Huang M *et al*. Postmenopausal obesity promotes tumor angiogenesis and breast cancer progression in mice. Cancer Biol Ther 2011; 11: 910-917.

4 Fukumura D, Incio J, Shankaraiah RC, Jain RK. Obesity and Cancer: An Angiogenic and Inflammatory Link. Microcirculation 2016; 23: 191-206.

5 Arendt LM, McCready J, Keller PJ, Baker DD, Naber SP, Seewaldt V *et al*. Obesity promotes breast cancer by CCL2-mediated macrophage recruitment and angiogenesis. Cancer Res 2013; 73: 6080-6093.

6 Jain RK. Antiangiogenesis strategies revisited: from starving tumors to alleviating hypoxia. Cancer Cell 2014; 26: 605-622.

7 Lohmann AE, Chia S. Patients with metastatic breast cancer using bevacizumab as a treatment: is there still a role for it? Curr Treat Options Oncol 2012; 13: 249-262.

8 Incio J, Ligibel JA, McManus DT, Suboj P, Jung K, Kawaguchi K *et al*. Obesity promotes resistance to anti-VEGF therapy in breast cancer by up-regulating IL-6 and potentially FGF-2. Science Translational Medicine 2018; 10.

9 Lei X, Shi F, Basu D, Huq A, Routhier S, Day R *et al*. Proteolytic processing of angiopoietin-like protein 4 by proprotein convertases modulates its inhibitory effects on lipoprotein lipase activity. J Biol Chem 2011; 286: 15747-15756.

10 Zhu P, Goh YY, Chin HF, Kersten S, Tan NS. Angiopoietin-like 4: a decade of research. Biosci Rep 2012; 32: 211-219.

11 Tan MJ, Teo Z, Sng MK, Zhu P, Tan NS. Emerging roles of angiopoietin-like 4 in human cancer. Mol Cancer Res 2012; 10: 677-688.

12 Padua D, Zhang XH, Wang Q, Nadal C, Gerald WL, Gomis RR *et al*. TGFbeta primes breast tumors for lung metastasis seeding through angiopoietin-like 4. Cell 2008; 133: 66-77.

13 Bai L, Wang F, Zhang DS, Li C, Jin Y, Wang DS *et al*. A plasma cytokine and angiogenic factor (CAF) analysis for selection of bevacizumab therapy in patients with metastatic colorectal cancer. Sci Rep 2015; 5: 17717.

14 Lichtenstein L, Mattijssen F, de Wit NJ, Georgiadi A, Hooiveld GJ, van der Meer R *et al*. Angptl4 protects against severe proinflammatory effects of saturated fat by inhibiting fatty acid uptake into mesenteric lymph node macrophages. Cell Metab 2010; 12: 580-592.

15 Gealekman O, Burkart A, Chouinard M, Nicoloro SM, Straubhaar J, Corvera S. Enhanced angiogenesis in obesity and in response to PPARgamma activators through adipocyte VEGF and ANGPTL4 production. Am J Physiol Endocrinol Metab 2008; 295: E1056-1064.

16 Choi J, Cha YJ, Koo JS. Adipocyte biology in breast cancer: From silent bystander to active facilitator. Prog Lipid Res 2018; 69: 11-20.

17 Bonny C, Oberson A, Negri S, Sauser C, Schorderet DF. Cell-permeable peptide inhibitors of JNK: novel blockers of beta-cell death. Diabetes 2001; 50: 77-82.

18 Vu BG, Gourronc FA, Bernlohr DA, Schlievert PM, Klingelhutz AJ. Staphylococcal superantigens stimulate immortalized human adipocytes to produce chemokines. PLoS One 2013; 8: e77988.

19 Hu K, Babapoor-Farrokhran S, Rodrigues M, Deshpande M, Puchner B, Kashiwabuchi F *et al*. Hypoxia-inducible factor 1 upregulation of both VEGF and ANGPTL4 is required to promote the angiogenic phenotype in uveal melanoma. Oncotarget 2016; 7: 7816-7828.

20 Goh YY, Pal M, Chong HC, Zhu P, Tan MJ, Punugu L *et al*. Angiopoietin-like 4 interacts with integrins beta1 and beta5 to modulate keratinocyte migration. Am J Pathol 2010; 177: 2791-2803.

21 Li L, Chong HC, Ng SY, Kwok KW, Teo Z, Tan EH *et al*. Angiopoietin-like 4 Increases Pulmonary Tissue Leakiness and Damage during Influenza Pneumonia. Cell Rep 2015.

22 DeCicco-Skinner KL, Henry GH, Cataisson C, Tabib T, Gwilliam JC, Watson NJ *et al*. Endothelial cell tube formation assay for the in vitro study of angiogenesis. J Vis Exp 2014: e51312.

23 Malinda KM. In vivo matrigel migration and angiogenesis assay. Methods Mol Biol 2009; 467: 287-294.

24 Li H, Ge C, Zhao F, Yan M, Hu C, Jia D *et al*. Hypoxia-inducible factor 1 alpha-activated angiopoietin-like protein 4 contributes to tumor metastasis via vascular cell adhesion molecule-1/integrin beta1 signaling in human hepatocellular carcinoma. Hepatology 2011; 54: 910-919.

25 Hata S, Nomura T, Iwasaki K, Sato R, Yamasaki M, Sato F *et al*. Hypoxia-induced angiopoietin-like protein 4 as a clinical biomarker and treatment target for human prostate cancer. Oncol Rep 2017.

26 Kim SH, Park YY, Kim SW, Lee JS, Wang D, DuBois RN. ANGPTL4 induction by prostaglandin E2 under hypoxic conditions promotes colorectal cancer progression. Cancer Res 2011; 71: 7010-7020.

27 Huang Z, Xie J, Lin S, Li S, Huang Z, Wang Y *et al*. The downregulation of ANGPTL4 inhibits the migration and proliferation of tongue squamous cell carcinoma. Arch Oral Biol 2016; 71: 144-149.

28 Tolaney SM, Boucher Y, Duda DG, Martin JD, Seano G, Ancukiewicz M *et al*. Role of vascular density and normalization in response to neoadjuvant bevacizumab and chemotherapy in breast cancer patients. Proc Natl Acad Sci U S A 2015; 112: 14325-14330.

29 Biswas T, Gu X, Yang J, Ellies LG, Sun LZ. Attenuation of TGF-beta signaling supports tumor progression of a mesenchymal-like mammary tumor cell line in a syngeneic murine model. Cancer Lett 2014; 346: 129-138.

30 Sugiura K, Stock CC. Studies in a tumor spectrum. I. Comparison of the action of methylbis (2-chloroethyl)amine and 3-bis(2-chloroethyl)aminomethyl-4-methoxymethyl -5-hydroxy-6-methylpyridine on the growth of a variety of mouse and rat tumors. Cancer 1952; 5: 382-402.

31 Tan W, Zhang W, Strasner A, Grivennikov S, Cheng JQ, Hoffman RM *et al*. Tumour-infiltrating regulatory T cells stimulate mammary cancer metastasis through RANKL-RANK signalling. Nature 2011; 470: 548-553.

32 O'Connell KA, Edidin M. A mouse lymphoid endothelial cell line immortalized by simian virus 40 binds lymphocytes and retains functional characteristics of normal endothelial cells. J Immunol 1990; 144: 521-525.

33 Markan KR, Naber MC, Ameka MK, Anderegg MD, Mangelsdorf DJ, Kliewer SA *et al*. Circulating FGF21 is liver derived and enhances glucose uptake during refeeding and overfeeding. Diabetes 2014; 63: 4057-4063.

34 Kuida K, Lippke JA, Ku G, Harding MW, Livingston DJ, Su MS *et al*. Altered cytokine export and apoptosis in mice deficient in interleukin-1 beta converting enzyme. Science 1995; 267: 2000-2003.

35 Lara-Tejero M, Sutterwala FS, Ogura Y, Grant EP, Bertin J, Coyle AJ *et al*. Role of the caspase-1 inflammasome in Salmonella typhimurium pathogenesis. J Exp Med 2006; 203: 1407-1412.

36 Zudaire E, Gambardella L, Kurcz C, Vermeren S. A computational tool for quantitative analysis of vascular networks. PLoS One 2011; 6: e27385.

37 Goecks J, Nekrutenko A, Taylor J, Galaxy T. Galaxy: a comprehensive approach for supporting accessible, reproducible, and transparent computational research in the life sciences. Genome Biol 2010; 11: R86.

38 Blankenberg D, Von Kuster G, Coraor N, Ananda G, Lazarus R, Mangan M *et al*. Galaxy: a web-based genome analysis tool for experimentalists. Curr Protoc Mol Biol 2010; Chapter 19: Unit 19 10 11-21.

39 Giardine B, Riemer C, Hardison RC, Burhans R, Elnitski L, Shah P *et al*. Galaxy: a platform for interactive large-scale genome analysis. Genome Res 2005; 15: 1451-1455.

40 Trapnell C, Roberts A, Goff L, Pertea G, Kim D, Kelley DR *et al*. Differential gene and transcript expression analysis of RNA-seq experiments with TopHat and Cufflinks. Nat Protoc 2012; 7: 562-578.

41 Gyorffy B, Lanczky A, Eklund AC, Denkert C, Budczies J, Li Q *et al*. An online survival analysis tool to rapidly assess the effect of 22,277 genes on breast cancer prognosis using microarray data of 1,809 patients. Breast Cancer Res Treat 2010; 123: 725-731.

42 Uhlen M, Fagerberg L, Hallstrom BM, Lindskog C, Oksvold P, Mardinoglu A *et al*. Proteomics. Tissue-based map of the human proteome. Science 2015; 347: 1260419.

Figure Legends

Figure 1. NLRC4-inflammasome upregulates ANGPTL4 in tumors from diet-induced obese mice

A) Heatmap showing differentially regulated genes in tumors from diet-induced obese mice that are NLRC4-dependent. Next generation RNA sequencing was performed using tumor RNAs from WT mice fed a normal diet (WT ND), WT mice fed a high-fat diet (WT HFD), or *Nlrc4*$^{-/-}$ mice fed a HFD (*Nlrc4*$^{-/-}$ HFD). Each lane represents a combination of equal amount of RNAs from 3 individual tumors.

B, C) Average *Angptl4* mRNA relative to *Ppia* in tumors from the indicated mice presented as a fold change compared to WT ND. (n=3 for all groups)

One-way ANOVA with multiple comparisons correction using Dunnett's test was performed to determine significance in B-C.

Figure 2. ANGPTL4 promotes tumor growth and angiogenesis in obese mice

A, B) *Angptl4*$^{+/-}$ and *Angptl4*$^{-/-}$ littermates were fed either a normal diet (ND) or high fat diet (HFD) for 10 weeks, followed by implantation of $1x10^5$ Py8119 cells into the #4 mammary fatpad. Graphs depict the average body weight ±s.e.m. (A) and tumor volumes (B) ± s.e.m. from the indicated mice (n=5 *Angptl4*$^{-/-}$ ND; n=6 *Angptl4*$^{-/-}$ HFD; n=6 *Angpt4l*$^{+/-}$ ND; n=8 *Angptl4*$^{+/-}$ HFD).

C) The indicated mice were given an ND or HFD for 10 weeks and then implanted with $1x10^5$ E0771 cells. Graph depicts the average tumor volumes ± s.e.m. for the indicated mice (n=5 for all groups).

D-E) IHC staining of CD31 from tumors used in Figure 2B. (D) Representative images from the indicated mice. Scale bars: 200 μm. (E) Average CD31-positive ± s.d. staining as a percent of total pixels in tumors from the indicated mice (At least 4 fields per sample and 3 samples per group were quantified).

F-G) IHC staining of CD34 from tumors used in Figure 2B. (F) Representative images from the indicated mice. Scale bars: 200 μm. (G) Average CD34-positive ± s.d. staining in tumors from the indicated mice (At least 4 fields per sample and 3 samples per group were quantified).

H-I) IHC staining of CD31 from tumors used in Figure 2C. (H) Representative images from the indicated mice. Scale bars: 200 μm. (I) Average CD31-positive ± s.d. staining in tumors from the indicated mice (At least 4 fields per sample and 3 samples per group were quantified).

Two-way ANOVA was used to determine significance in A-C. One-way ANOVA with multiple comparisons correction using Dunnett's test was performed to determine significance in E, G, and I.

Figure 3. IL-1β directly upregulates ANGPTL4 in adipocytes

A) The indicated cells were treated with 100 ng/ml IL-1β for 6 hours. Graph depicts the average *Angptl4* mRNA relative to *Ppia* ± s.d. (n=3 for all groups).

B) Human preadipocytes were differentiated into adipocytes and treated with 100 ng/ml of IL-1β for 4 hours. Then the media was collected and cells were lysed. Immunoblots for ANGPTL4 is shown. β-ACTIN was included as a loading control.

C) Primary mouse adipocytes were treated as indicated. Graph depicts the average *Angptl4* mRNA relative to *Ppia* ± s.d. as a fold change compared to control (n=3 for all groups).

D) Primary mouse adipocytes were treated with 30 μM D-JNKi or control peptide 1 hour prior to treatment with 100 ng/ml IL-1β for 6 hours. Graph depicts the average *Angptl4* mRNA relative to *Ppia* ± s.d. (n=3 for all groups).

E) Differentiated human adipocytes were transduced with adenovirus expressing GFP (Ad-GFP), dominant-negative JNK (Ad-DN-JNK) or dominant-negative IKKβ (Ad-DN-IKKβ) for 16 hours then treated with 100 ng/ml IL-1β for 6 hrs. Graph depicts the average *ANGPTL4* mRNA relative to *ACTB* ± s.d. (n=3 for all groups).

F) Primary adipocytes were treated with or without IL-1β and incubated at 20% or 1% O_2 for 6 hours. Graph depicts the average *Angptl4* mRNA relative to *Ppia* ± s.d. as a fold change compared to control (n=3 for all groups).

G) Immortalized human preadipocytes were differentiated into mature adipocytes then treated as in C. Graph depicts the average *ANGPTL4* mRNA relative to *PPIA* ± s.d. as a fold change compared to control (n=3 for all groups).

In (C, D and F) data depicts the results of a single experiment using adipocytes from one litter of mice treated in triplicate. Experiments were repeated using different batches of adipocytes with similar results. One-way ANOVA with multiple comparisons correction using Dunnett's test was performed to determine significance.

Figure 4. ANGPTL4 in human obesity and breast cancer.

A) Box plots depicting *ANGPTL4* mRNA with 95% confidence interval (CI) in normal mammary tissue in normal weight (BMI<25), overweight (BMI 25-30) and obese (BMI>30) patients. Data were from GSE33256. Number of samples is indicated. Welch's t-test was used to determine significance.

B, C) Correlation between *ANGPTL4* mRNA and recurrence-free survival (RFS) in all breast cancer samples (B) and basal-like breast cancer (C). Data generated using KMplot meta-dataset of invasive ductal breast carcinoma. Number of cases and Log-rank P values are shown.

D) Mean centralized *ANGPTL4* mRNA with 95% CI in PAM50 subtypes of breast cancer. Data from TCGA invasive breast cancer cohort.

E) Correlation between *ANGPTL4* and *PECAM1* mRNA in basal like breast cancers. Data is from the basal-like breast cancer subtype of the TCGA invasive breast cancer cohort. Pearson r is indicated.

F) Gene Set Enrichment Analysis of basal-like breast cancer samples comparing *ANGPTL4* high expression tertile (n=66) to *ANGPTL4* low expression tertile (n=66) from GEO datasets GSE76275. Graph depicts the nominal

enrichment score (NES; bar) and FDRs (solid triangles) of a representative gene set related to the indicated pathway enriched in the *ANGPTL4* high tertile group. The number of pathways enriched related to the indicated pathways is labeled in parenthesis. Only gene sets with FDRs < 0.25 were considered significantly enriched.

G) Correlation between *VEGFA* and *ANGPTL4* mRNA in breast cancer samples from normal (BMI<25), overweight (BMI 25-30), and obese (BMI>30) patients from GSE20194. Pearson r is indicated.

Figure 5. Targeting cANGPTL4 inhibits obesity-driven cancer progression and angiogenesis.

A) WT mice were fed and implanted with Py8119 cells as described in Figure 2. Mice were treated with anti-cANGPTL4 antibody (Ab) or rabbit IgG twice weekly once tumors were palpable. Graph depicts the average tumor volumes ± s.e.m. from the indicated mice (n=5 for all groups except ND IgG, n=4). Two-way ANOVA was used to determine significance.

B-C) IHC staining for CD31 from tumors used in Figure 5A. (B) Representative images from the indicated mice. Scale bars: 200 μm. (C) Average CD31-positive staining ± s.d. as a percent of total pixels in tumors from the indicated mice (At least 4 fields per sample and 3 samples per group were quantified). One-way ANOVA with multiple comparisons correction using Dunnett's test was performed to determine significance

D-E) Endothelial cell tube formation assay. Endothelial cells were plated on matrigel and treated as indicated. 6 hour later cells were stained with Calcein AM and imaged (D). Images were analyzed and total tube length was determined. Graph (E) depicts the average total tube length ± s.d. (n=3 for all groups). One-way ANOVA with multiple comparisons correction using Dunnett's test was performed to determine significance.

F-G) Matrigel plug assay. Athymic nude mice were implanted with matrigel containing the indicated doses of recombinant human cANGPTL4 and 48 ng/ml anti-cANGPTL4 antibody or rat IgG. After 6 days, the matrigel plugs were removed and hemoglobin was measured as a redout for angiogenesis. Representative images (F) are shown. Graph (G) depicts the average hemoglobin concentration ± s.d. (n=6 for all groups).

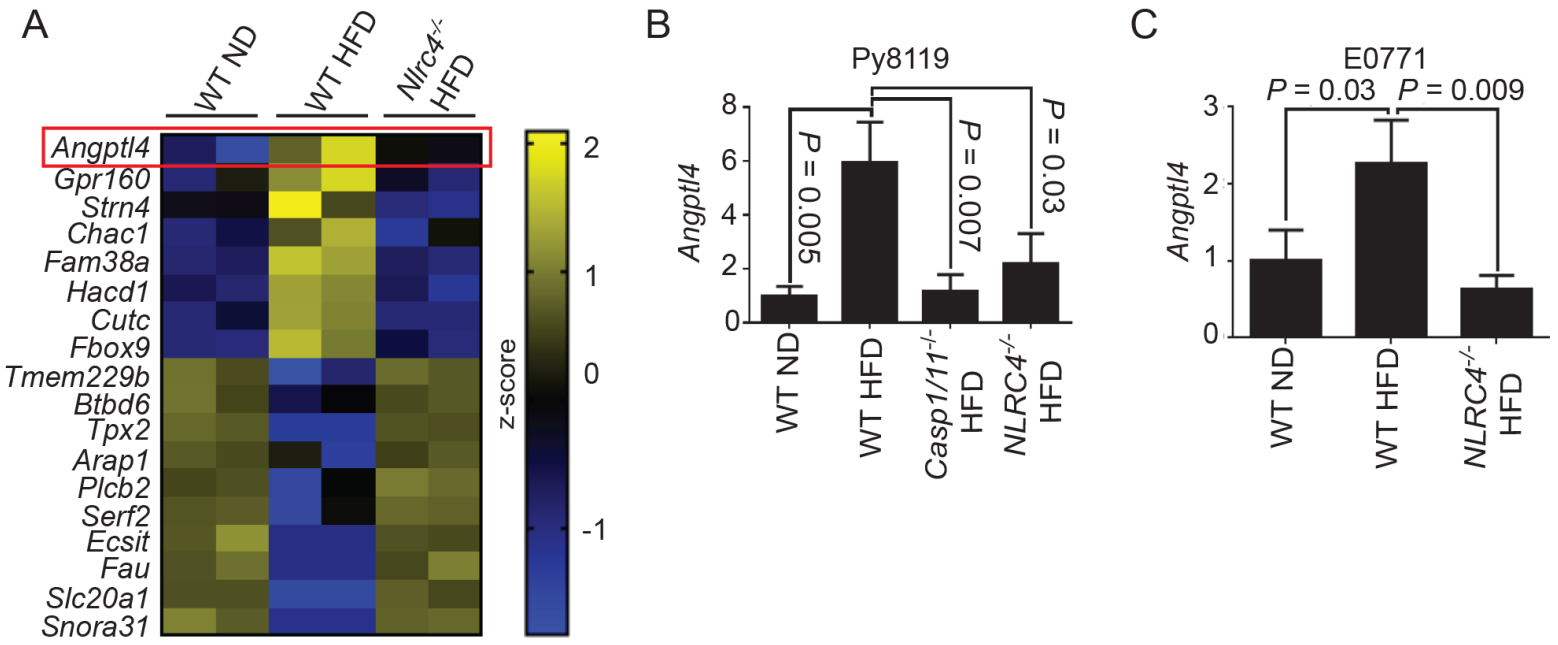
A
WT ND
WT HFD
Nlrc4-/- HFD
Angptl4
Gpr160
Strn4
Chac1
Fam38a
Hacd1
Cutc
Fbox9
Tmem229b
Btbd6
Tpx2
Arap1
Plcb2
Serf2
Ecsit
Fau
Slc20a1
Snora31
z-score
2
1
0
-1
B
Py8119
Angptl4
P = 0.005
P = 0.007
P = 0.03
WT ND
WT HFD
Casp1/11-/- HFD
NLRC4-/- HFD
C
E0771
P = 0.03
P = 0.009
Angptl4
WT ND
WT HFD
NLRC4-/- HFD

Figure 1.

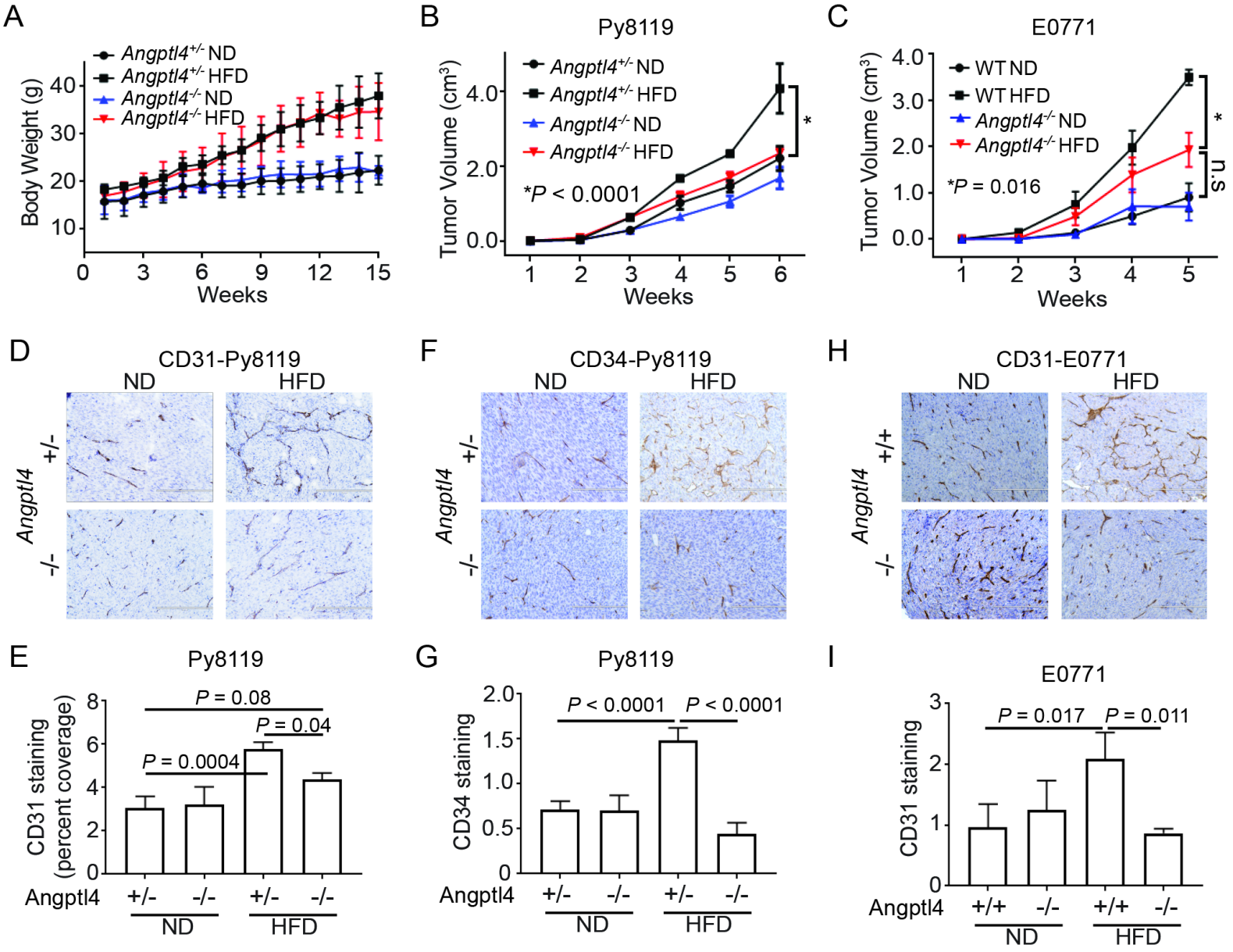
A
Body Weight (g)
Weeks
Angptl4+/- ND
Angptl4+/- HFD
Angptl4-/- ND
Angptl4-/- HFD
B
Py8119
Tumor Volume (cm3)
Weeks
*P < 0.0001
*
C
E0771
Tumor Volume (cm3)
Weeks
WT ND
WT HFD
Angptl4-/- ND
Angptl4-/- HFD
*P = 0.016
*
n.s
D
CD31-Py8119
ND
HFD
Angptl4
+/-
-/-
F
CD34-Py8119
ND
HFD
Angptl4
+/-
-/-
H
CD31-E0771
ND
HFD
Angptl4
+/+
-/-
E
Py8119
CD31 staining (percent coverage)
P = 0.08
P = 0.04
P = 0.0004
Angptl4
+/-
-/-
+/-
-/-
ND
HFD
G
Py8119
CD34 staining
P < 0.0001
P < 0.0001
Angptl4
+/-
-/-
+/-
-/-
ND
HFD
I
E0771
CD31 staining
P = 0.017
P = 0.011
Angptl4
+/+
-/-
+/+
-/-
ND
HFD

Figure 2.

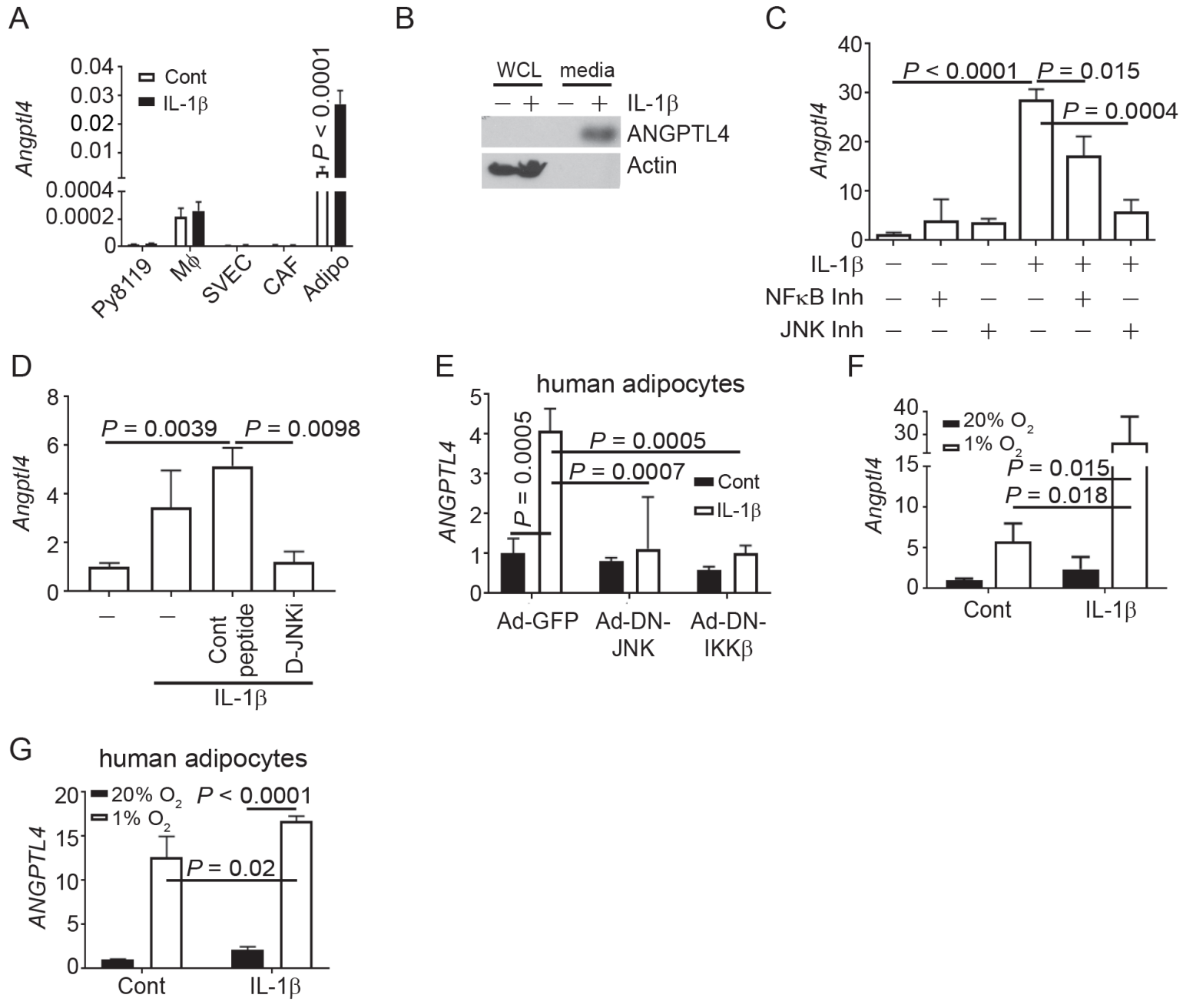
A
Angptl4
Cont
IL-1β
P < 0.0001
Py8119
Mϕ
SVEC
CAF
Adipo
B
WCL
media
IL-1β
ANGPTL4
Actin
C
Angptl4
P < 0.0001
P = 0.015
P = 0.0004
IL-1β
NFκB Inh
JNK Inh
D
Angptl4
P = 0.0039
P = 0.0098
Cont peptide
D-JNKi
IL-1β
E
human adipocytes
ANGPTL4
P = 0.0005
P = 0.0007
P = 0.0005
Cont
IL-1β
Ad-GFP
Ad-DN-JNK
Ad-DN-IKKβ
F
Angptl4
20% O2
1% O2
P = 0.015
P = 0.018
Cont
IL-1β
G
human adipocytes
ANGPTL4
20% O2
1% O2
P < 0.0001
P = 0.02
Cont
IL-1β

Figure 3.

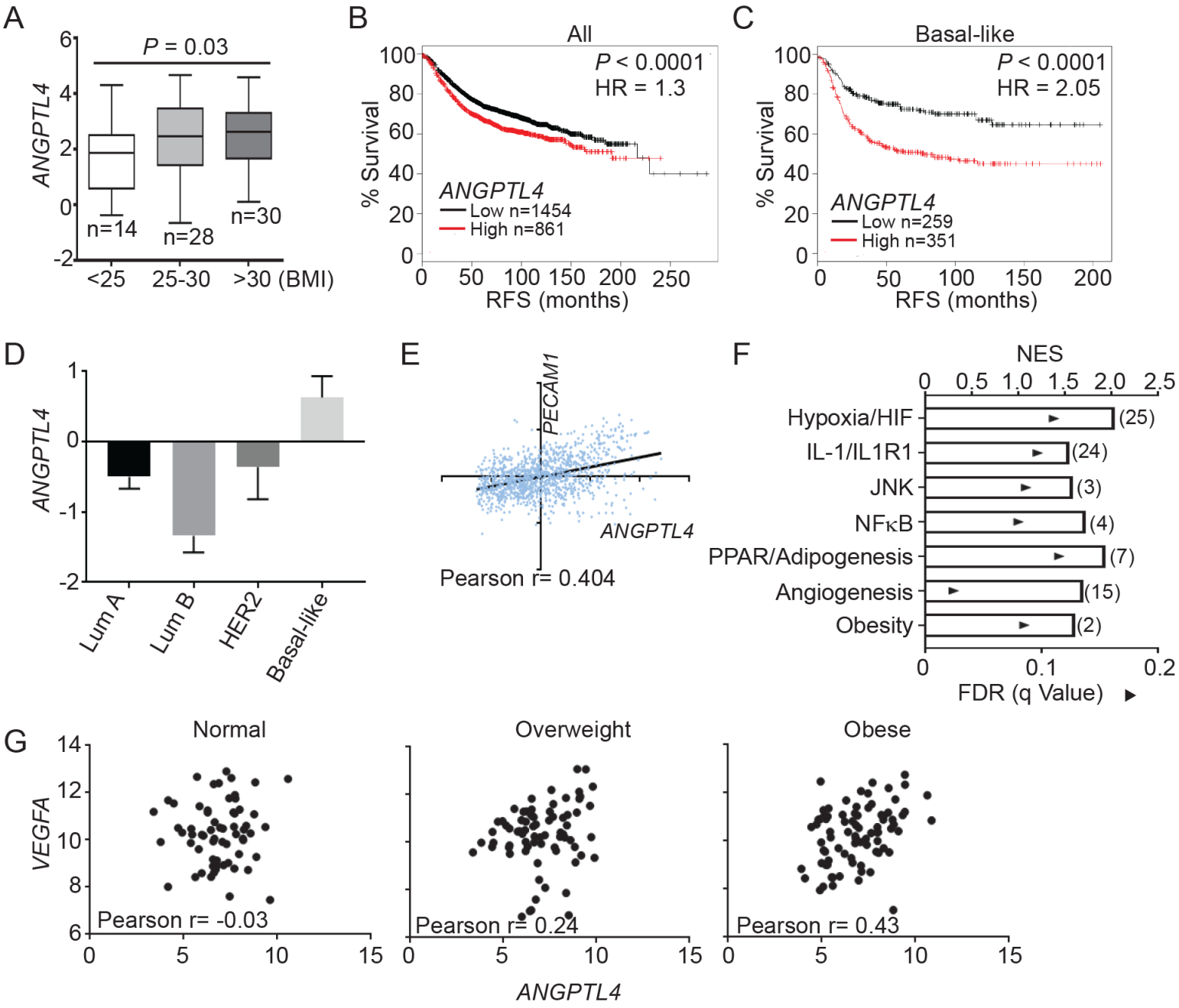
A
P = 0.03
ANGPTL4
n=14
n=28
n=30
<25
25-30
>30 (BMI)
B
All
P < 0.0001
HR = 1.3
% Survival
ANGPTL4
Low n=1454
High n=861
RFS (months)
C
Basal-like
P < 0.0001
HR = 2.05
% Survival
ANGPTL4
Low n=259
High n=351
RFS (months)
D
ANGPTL4
Lum A
Lum B
HER2
Basal-like
E
PECAM1
ANGPTL4
Pearson r= 0.404
F
NES
Hypoxia/HIF
IL-1/IL1R1
JNK
NFκB
PPAR/Adipogenesis
Angiogenesis
Obesity
(25)
(24)
(3)
(4)
(7)
(15)
(2)
FDR (q Value)
G
Normal
Overweight
Obese
VEGFA
Pearson r= -0.03
Pearson r= 0.24
Pearson r= 0.43
ANGPTL4

Figure 4.

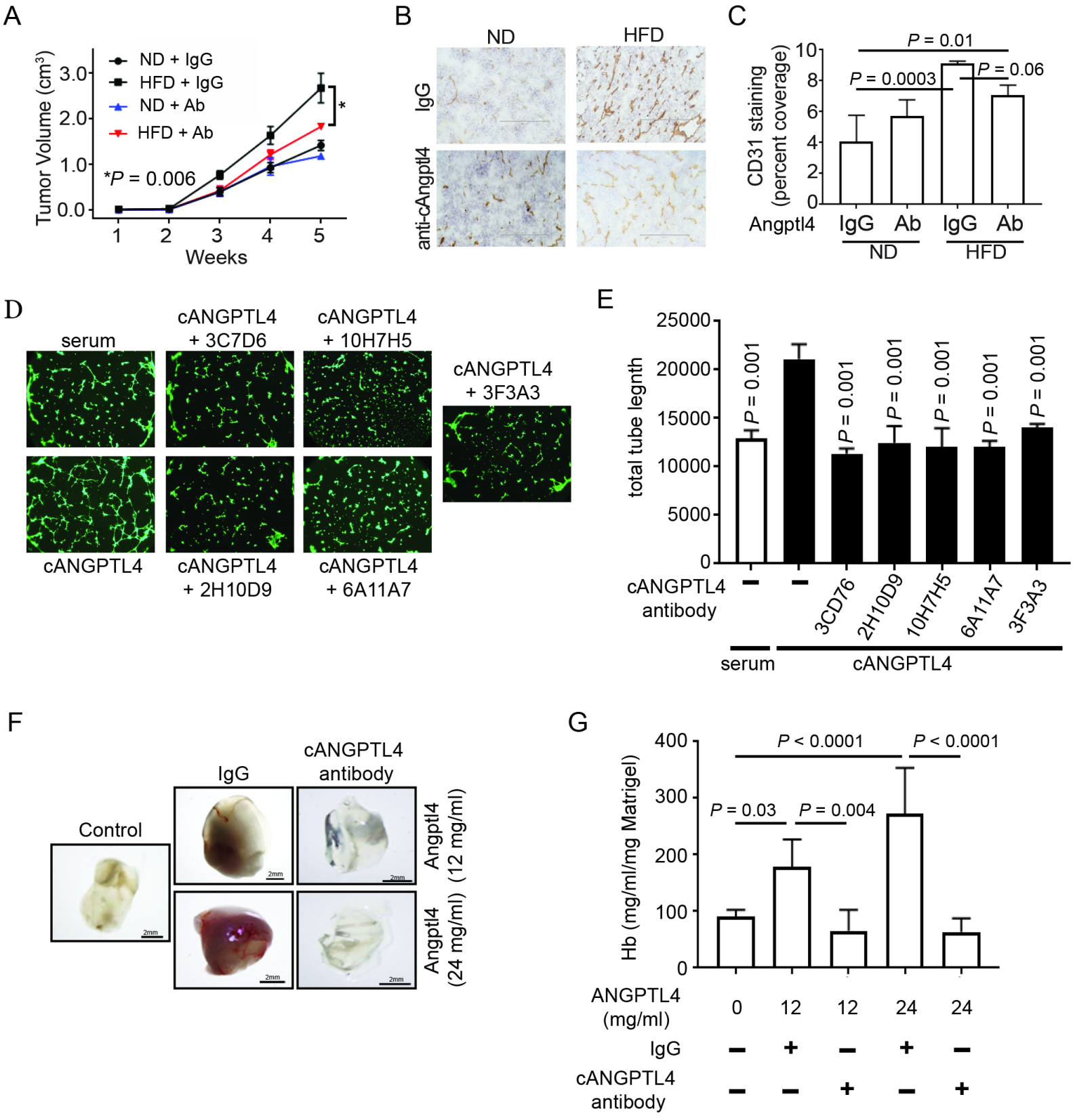
A
Tumor Volume (cm³)
ND + IgG
HFD + IgG
ND + Ab
HFD + Ab
*P = 0.006
Weeks
B
ND
HFD
IgG
anti-cAngptl4
C
CD31 staining (percent coverage)
P = 0.01
P = 0.0003
P = 0.06
Angptl4
IgG
Ab
IgG
Ab
ND
HFD
D
serum
cANGPTL4 + 3C7D6
cANGPTL4 + 10H7H5
cANGPTL4 + 3F3A3
cANGPTL4
cANGPTL4 + 2H10D9
cANGPTL4 + 6A11A7
E
total tube legnth
P = 0.001
cANGPTL4 antibody
3CD76
2H10D9
10H7H5
6A11A7
3F3A3
serum
cANGPTL4
F
Control
IgG
cANGPTL4 antibody
Angptl4 (12 mg/ml)
Angptl4 (24 mg/ml)
2mm
G
Hb (mg/ml/mg Matrigel)
P < 0.0001
P < 0.0001
P = 0.03
P = 0.004
ANGPTL4 (mg/ml)
0
12
12
24
24
IgG
cANGPTL4 antibody

Figure 5.